Electronic Supplementary Information

Mn single atom catalyst with Mn-N_2O_2 sites integrated into carbon nanosheets for efficient electrocatalytic CO_2 reduction

Wenfei Dong [1], Nan Zhang[1], Sanxiu Li [1], Shixiong Min[2], Juan Peng [1*], Wanyi Liu [1*], Dongping Zhan [3], Hongcun Bai[1]

[1] School of Chemistry and Chemical Engineering, State Key Laboratory of High-efficiency Utilization of Coal and Green Chemical Engineering, Ningxia University, Yinchuan, Ningxia, 750021, P.R. China.

[2]School of Chemistry and Chemical Engineering, North Minzu University, Yinchuan,750021, P. R. China.

[3]Department of Chemistry, College of Chemistry and Chemical Engineering; and Department of Mechanical and Electrical Engineering, School of Aerospace Engineering, Xiamen University, Xiamen 361005, China.

**Corresponding author: pengjuan@nxu.edu.cn; liuwy@nux.edu.cn.*

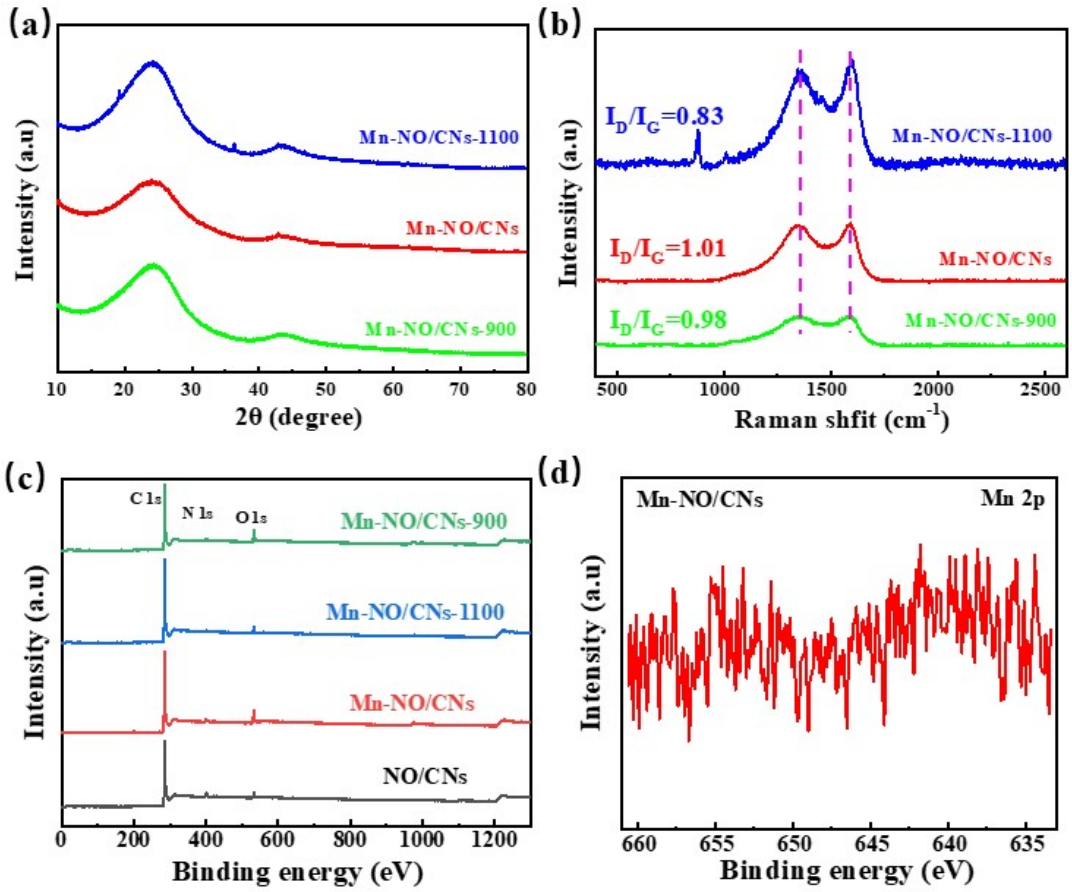

Figure S1. (a) XRD, (b)Raman spectra, (c) XPS survey spectra of NO/CNs, Mn-NO/CNs-1100, Mn-NO/CNs, and Mn-NO/CNs-900, (d) XPS Mn 2p spectrum of Mn-NO/CNs.

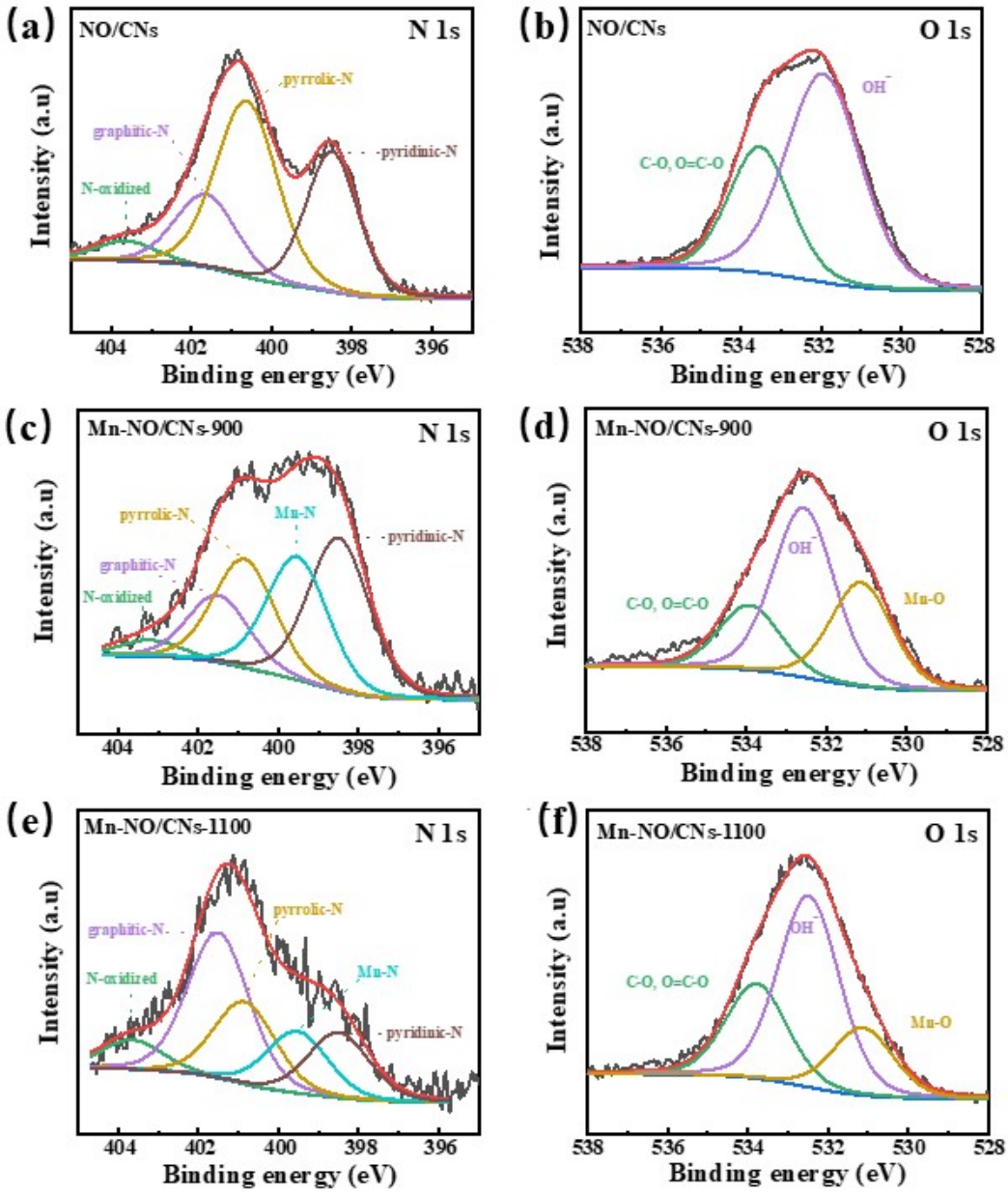

Figure S2. XPS N 1s spectrum of (a) NO/CNs, (c) Mn-NO/CNs-900, and (e) Mn-NO/CNs-1100; XPS O 1s spectrum of (b) NO/CNs, (d) Mn-NO/CNs-900, and (f) Mn-NO/CNs-1100.

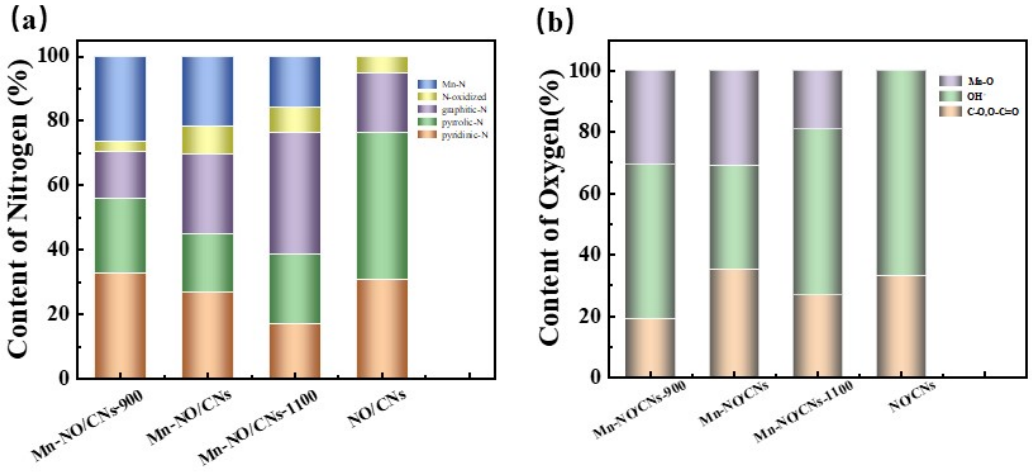

Figure S3. The corresponding atomic percentage of different N-substance (a) and O-species (b) fitted according to the XPS curve of the sample.

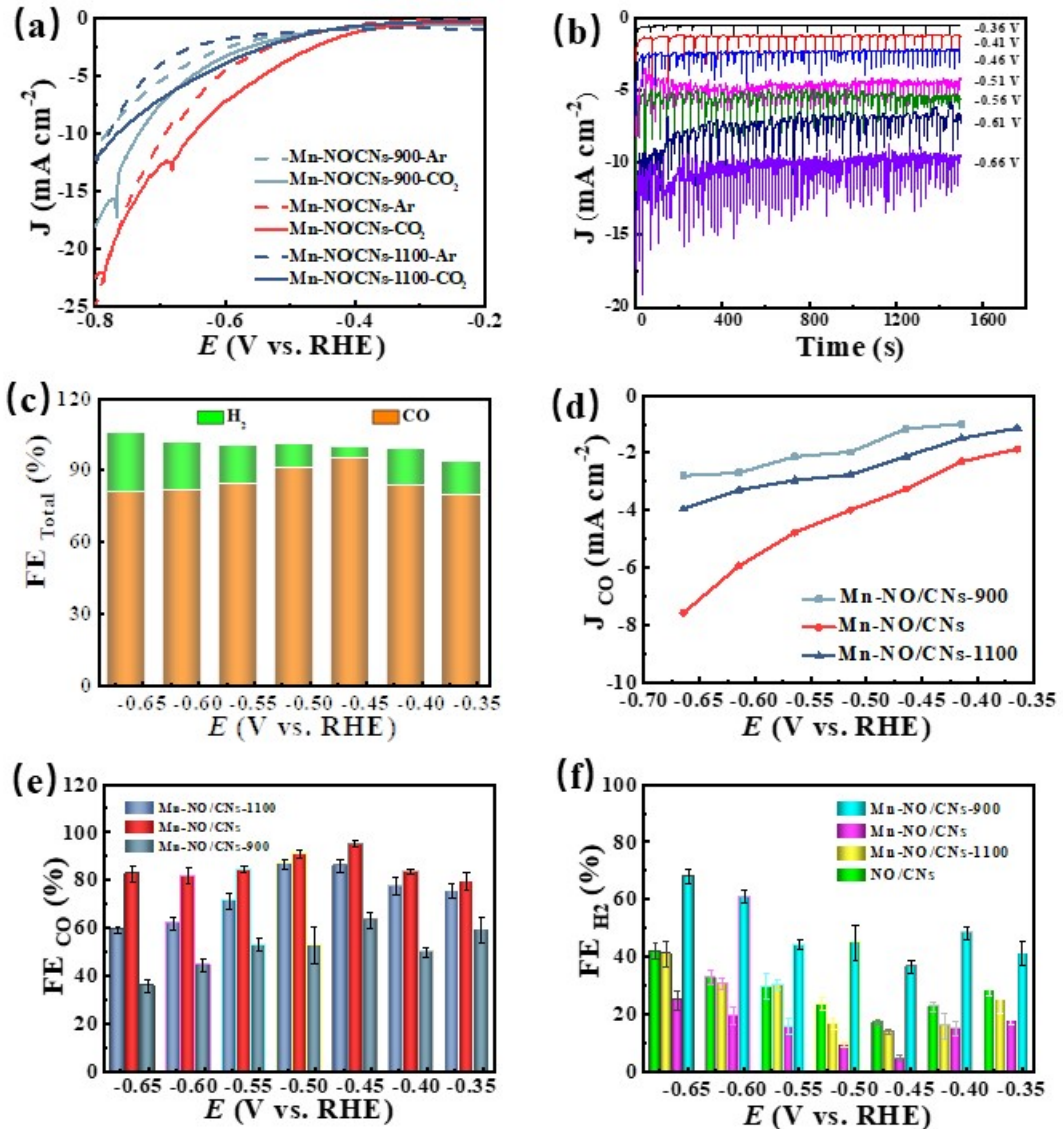

Figure S4. (a) LSV curves of Mn-NO/CNs-900, Mn-NO/CNs, and Mn-NO/CNs -1100 the catalysts on carbon paper in Ar- or CO_2-saturated 0.5 M $KHCO_3$ solution at the scan rate of 5 mV s^{-1}, with a catalyst loading of 0.56 mg cm^{-2}. (b) Current response of Mn-NO/CNs in 0.5 M $KHCO_3$ saturated with CO_2; (c) Total FE of Mn-NO/CNs catalyst at different potentials in an H-type electrolytic cell (0.5 M $KHCO_3$); (e) Potential dependent FE of CO formation; (f) Potential dependent FE of H_2 formation.

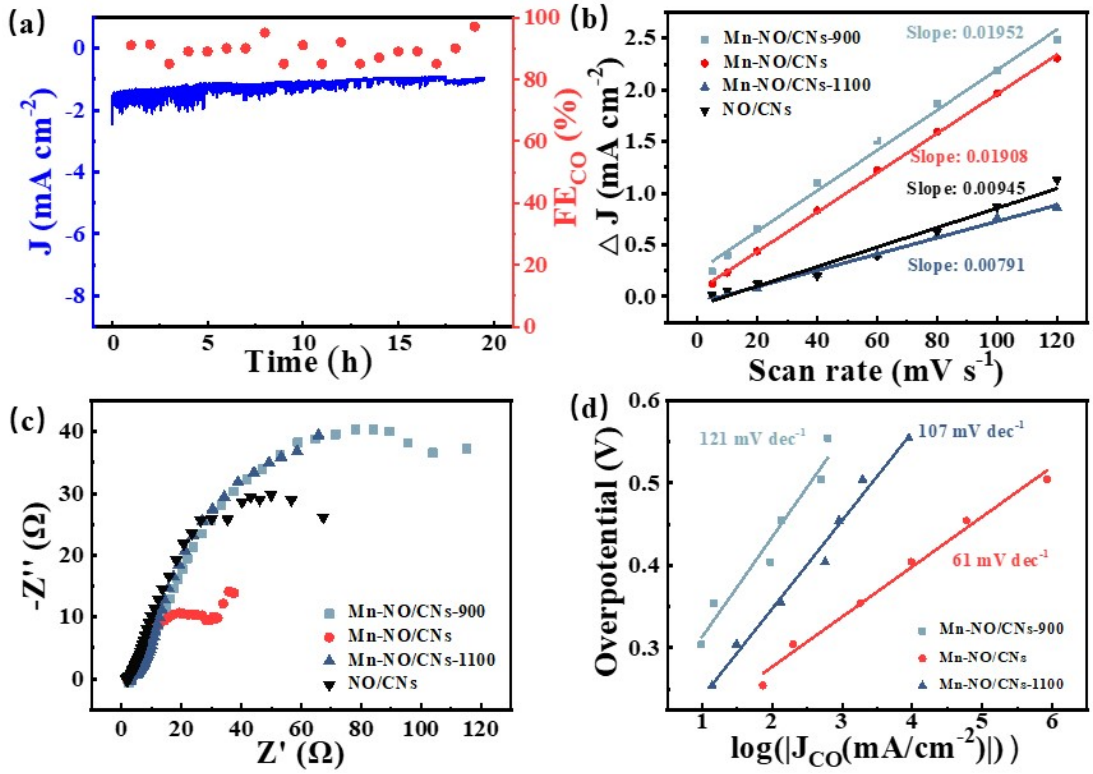

Figure S5. (a) Stability test of Mn-NO/CNs in H-type electrolytic cell (0.5 M $KHCO_3$ electrolyte) at −0.46 V (V vs. RHE); (b) The relationship between current density difference (△J) and scanning rate; (c) The impedance spectra of the catalyst at carbon paper obtained under CO_2RR (−0.46 V vs. RHE) condition (frequency range: 0.1 MHz~10^{-2} Hz); (d) Tafel diagrams.

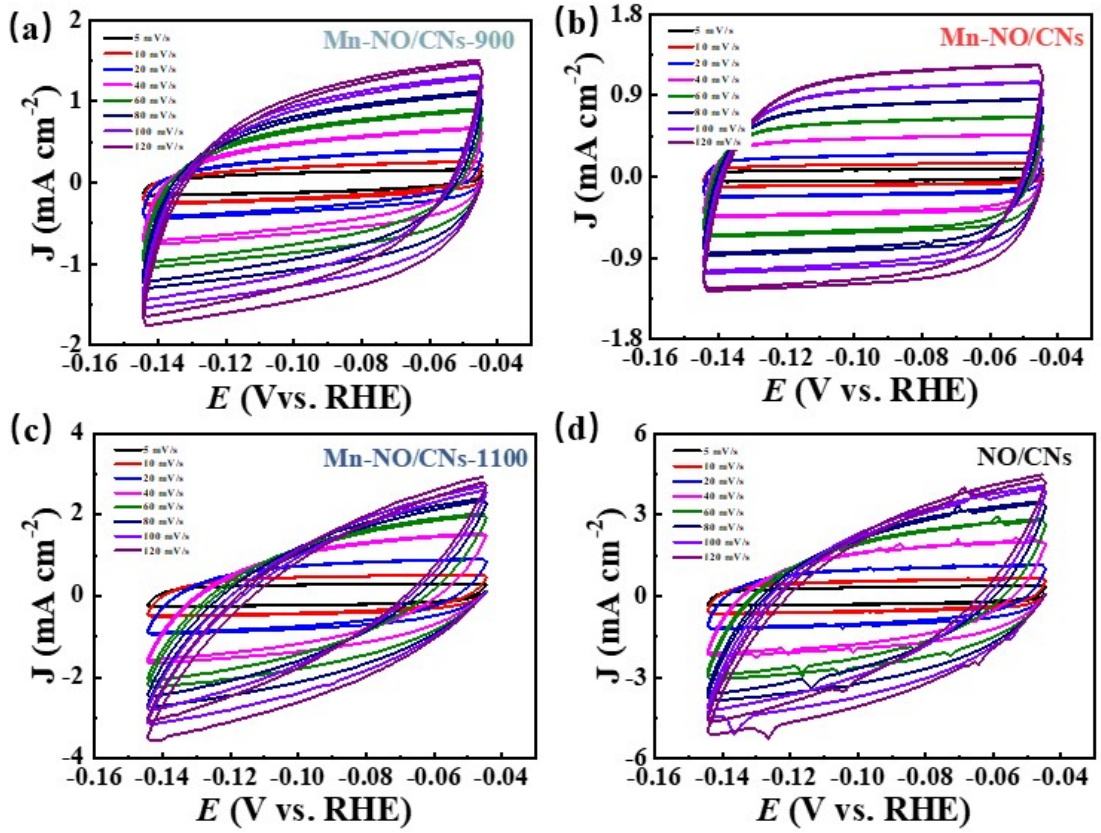

Figure S6. Cycle voltammetry curves of (a) Mn-NO/CNs-900, (b) Mn-NO/CNs, (c) Mn-NO/CNs-1100 and (d) NO/CNs.

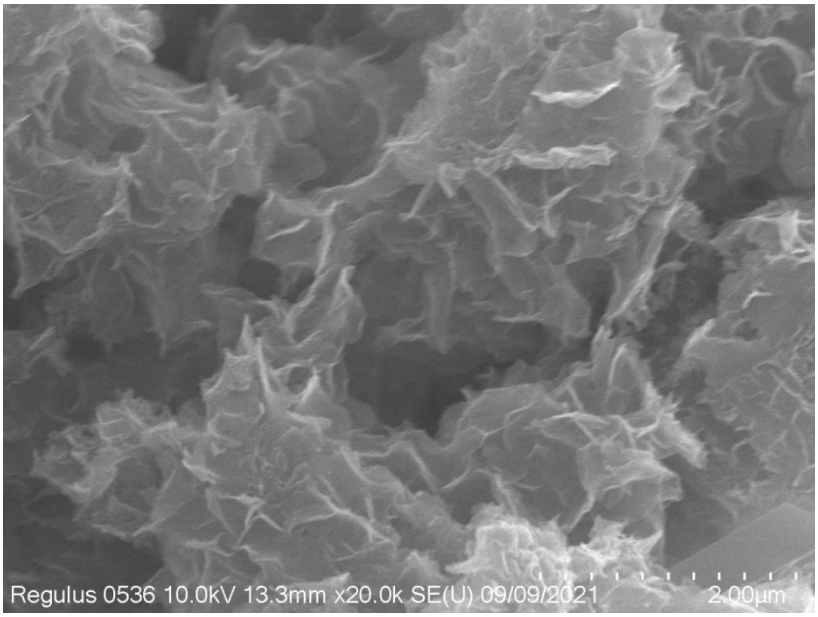

Figure S7. SEM image of Mn-NO/CNs catalyst after 70 hours of electrolysis.

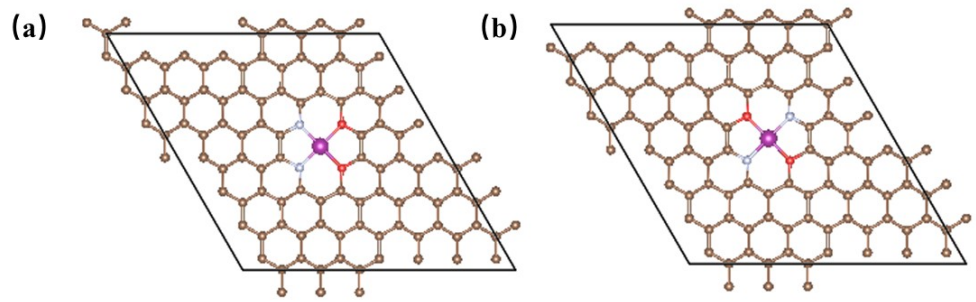

Figure S8. Top view configurations of two Mn-N_2O_2 types. The gray, blue, purple, and red spheres represent C, N, Mn, and O atoms, respectively.

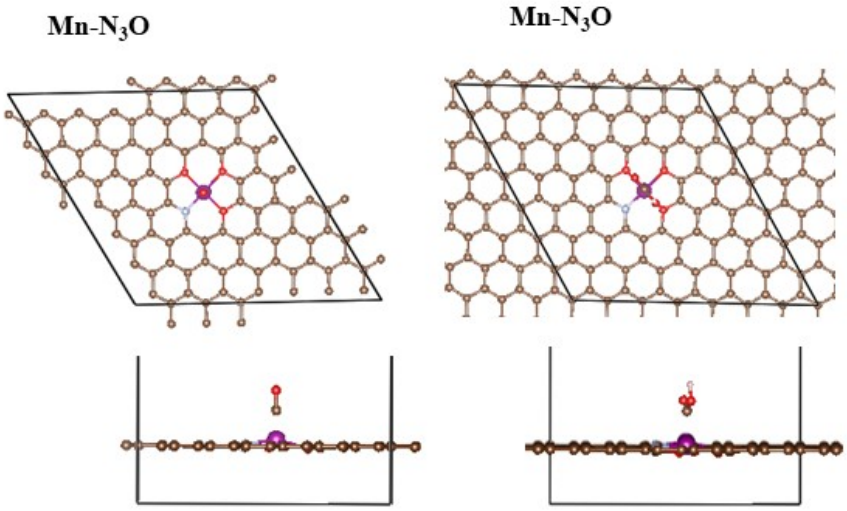

Figure S9. The adsorption configuration of *CO and *COOH on Mn-N_3O. The gray, blue, purple, and red spheres represent C, N, Mn, and O atoms, respectively.

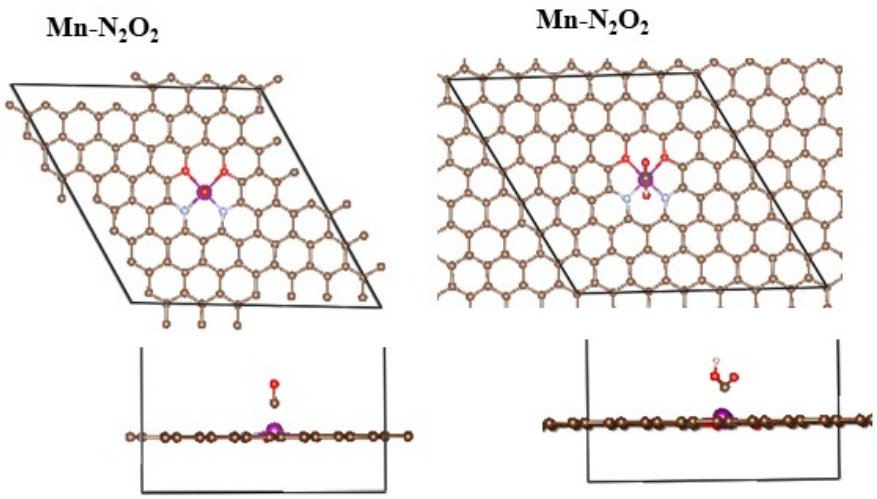

Figure S10. The adsorption configuration of *CO and *COOH on Mn-N_2O_2. The gray, blue, purple, and red spheres represent C, N, Mn, and O atoms, respectively.

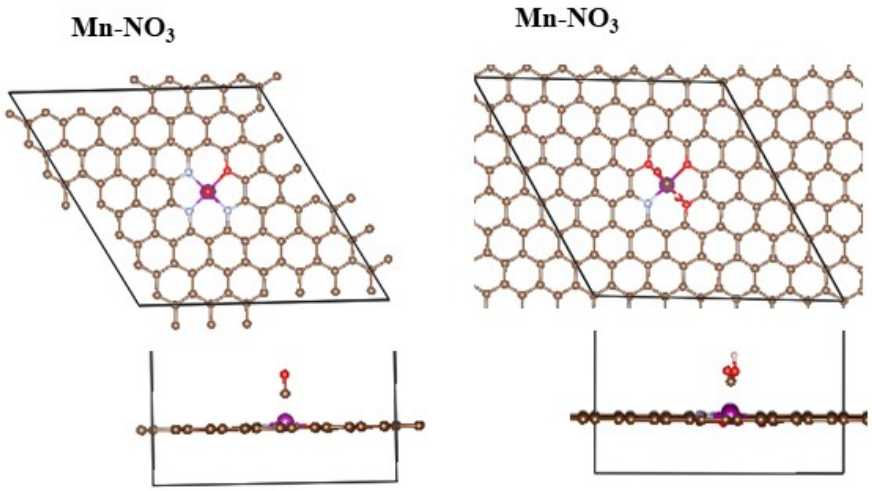

Figure S11. The adsorption configuration of *CO and *COOH on Mn-NO_3. The gray, blue, purple, and red spheres represent C, N, Mn, and O atoms, respectively.

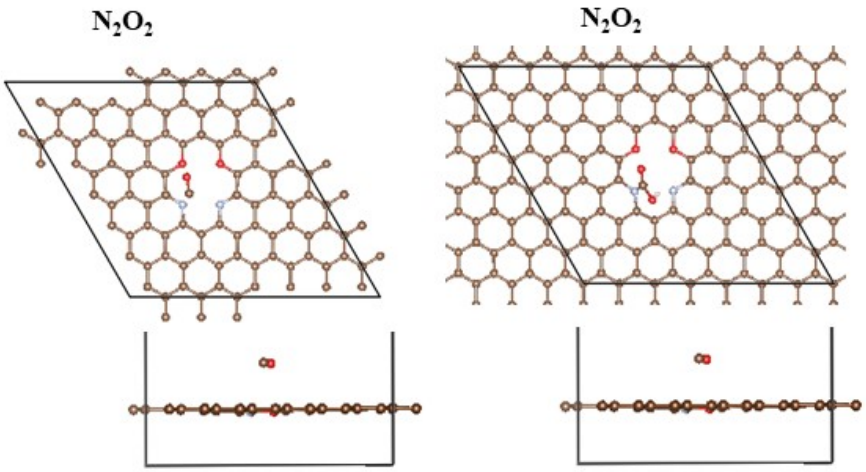

Figure S12. The adsorption configuration of *CO and *COOH on N_2O_2. The gray, blue, purple, and red spheres represent C, N, Mn, and O atoms, respectively.

Supplementary Tables

Table S1. X-ray photoelectron spectrum analysis of the Mn-NO/CNs-900, Mn-NO/CNs, Mn-NO/CNs-1100 and NO/CNs.

Catalysts	Element content/%(at%)		
	C at %	N at %	O at %
Mn-NO/CNs-900	86.66	4.51	8.82
Mn-NO/CNs	87.12	4.23	8.30
Mn-NO/CNs-1100	93.01	2.46	4.52
NO/CNs	90.29	5.88	3.83

Table S2. The peak quantification of XPS fitted N1s and O 1s spectra of the Mn-NO/CNs-900, Mn-NO/CNs-1000, Mn-NO/CNs-1100 and NO/CNs-1000.

Catalysts	Fitting of N moieties/atom %					Fitting of O moieties/atom%		
	pyridinic-N at %	pyrrolic-N at %	graphitic-N at %	N-oxidized at %	Mn-N at %	C-O, O=C-O	OH	Mn-O
Mn-NO/CNs-900	32.60	23.21	14.38	3.49	26.30	19.15	50.18	30.67
Mn-NO/CNs	26.54	18.17	24.68	8.88	21.73	35.20	33.80	31.00
Mn-NO/CNs-1100	17.00	21.44	37.82	7.67	16.06	26.79	35.35	19.11
NO/CNs	30.75	45.30	18.77	5.17	0	33.1	66.9	0

Table S3. EXAFS fitting results of Mn-NO/CNs.

S_0^2=0.73

	shell	CN	R(Å)	σ^2	ΔE_0	R factor
MnO	Mn-O	6	2.19±0.01	0.0076	0.4±1.1	0.0072
	Mn-Mn	6	3.09±0.01	0.0047		
	Mn-Mn1	6	3.19±0.01	0.0046		
sample	Mn-NO/CNs	3.7±0.6	2.18±0.04	0.0052	1.2±3.3	0.0150

[a]*N*: coordination numbers; [b]*R*: bond distance; [c]σ^2: Debye-Waller factors; [d] ΔE_0: the inner potential correction. *R* factor: goodness of fit. S_0^2 was set to 0.70, according to the experimental EXAFS fit of Fe foil reference by fixing CN as the known crystallographic value; δ: percentage.

Table S4. Comparison of the Performance of Mn-NO/CNs with Other Single Atom Catalysts and Supported Molecular Complexes for CO_2RR.

Catalyst	Electrolyte	Potential for FE_{max} (vs. RHE)	CO maximum FE	Stability (h)	Ref.
Fe/NG	0.1 M $KHCO_3$	−0.60 V	80.0%	10	[1]
DNG-SAFe	0.1 M $KHCO_3$	−0.75 V	90.0%	20	[2]
Fe-N/O-doped carbon	0.1 M $KHCO_3$	−0.57 V	96.0 %	22	[3]
Mn–C_3N_4/CNT	0.5 M $KHCO_3$	−0.44 V	98.8%	20	[4]
(Cl, N)-Mn/G	0.5 M $KHCO_3$	−0.49 V	97.0%	12	[5]
CoN_5/HNPCSs	0.5 M $KHCO_3$	−0.49 V	94.0%	10	[6]
Bi SAs/NC	0.1 M $NaHCO_3$	−0.39 V	97.0%	4	[7]
Cu SAs/NC	0.1 M $KHCO_3$	−0.70V	92.0%	30	[8]
Ni-N_3-C	0.5 M $KHCO_3$	−0.65V	95.6%	10	[9]
ACP/S-N-Ni	0.5 M $KHCO_3$	−0.77 V	91.0%	14	[10]
Ni SAs/N-C	0.5 M $KHCO_3$	−0.89 V	71.9%	-	[11]
FeNPCN	0.1 M $KHCO_3$	−0.50 V	94.0%	12	[12]
Co_1-N_4	0.1M $KHCO_3$	−0.80 V	82.0%	10	[13]
Ni_1-N-C	0.5M $KHCO_3$	−0.80 V	96.8%	10	[14]
Mn-NO/CNs	**0.5 M $KHCO_3$**	**−0.46 V**	**96.0%**	**20**	**This work**

Fe/NG: atomic iron dispersed on nitrogen-doped graphene; DNG-SAFe: intrinsic defect-rich graphene-like porous carbon embedded with single-atom Fe–N_4 sites; g-C_3N_4: graphitic carbon nitride; CNTs: carbon nanotubes; G: graphene; HNPCSs: hollow N-doped porous carbon spheres; Bi SAs/NC: single Bi atoms on N-doped carbon networks; Cu SAs/ NC: single Cu atoms dispersed on N-doped carbon substrate; ACP: activated carbon paper; FeNPCN: Fe and N doping porous carbon nematosphere; Co_1-N_4: four-coordinated N on N-doped porous carbon; Ni_1-N-C: single-atom metals implanted in N-doped carbon.

Table S5. DFT total energy (E_{DFT}), zero-point energy (ZPE), entropy multiplied by temperature (TΔS, T = 300 K), and free energy (G) for CO_2, H_2, H_2O, and CO.

	E_{DFT}（eV）	ZPE	TS	G
CO_2	−23.00	0.32	0.66	−23.34
CO	−14.80	0.14	0.61	−15.27
H_2	−6.76	0.28	0.40	−6.87
H_2O	−14.22	0.59	0.58	−14.22

Table S6. DFT total energy (E_{DFT}), zero-point energy (ZPE), entropy multiplied by temperature (TΔS, T = 300 K), and free energy (G) at U = 0 versus RHE and adsorption energies of CO_2 reduction reaction intermediates on Mn-NO_3, Mn-N_2O_2, Mn-N_3O and N_2O_2.

NO_3-Mn	E	ZPE	TS	G
*	−883.24			−883.24
*COOH	−910.10	0.61	0.18	−909.68
*CO	−899.69	0.21	0.13	−899.61
N_2O_2-Mn	E	ZPE	TS	G
*	−887.20			−887.20
*COOH	−913.94	0.61	0.21	−913.55
*CO	−903.35	0.21	0.15	−903.29
N_3O-Mn	E	ZPE	TS	G
*	−890.66			−890.66
*COOH	−917.36	0.62	0.22	−916.96
*CO	−906.82	0.21	0.15	−906.76
N_2O_2-pure	E	ZPE	TS	G
*	−878.58			−878.58
*COOH	−905.15	0.68	0.18	−904.65
*CO	−893.54	0.15	0.23	−893.61

References

1. C. Zhang, S. Yang, J. Wu, M. Liu, S. Yazdi, M. Ren, J. Sha, J. Zhong, K. Nie, A.S. Jalilov, Z. Li, H. Li, B.I. Yakobson, Q. Wu, E. Ringe, H. Xu, P.M. Ajayan and J.M. Tour, *Adv. Energy Mater.*, 2018, **8**, 1703487.
2. W. Ni, Z. Liu, Y. Zhang, C. Ma, H. Deng, S. Zhang and S. Wang, *Adv. Mater.*, 2021, **33**, 2003238.
3. X. Wang, Y. Pan, H. Ning, H. Wang, D. Guo, W. Wang, Z. Yang, Q. Zhao, B. Zhang, L. Zheng, J. Zhang and M. Wu, *Appl. Catal., B*, 2020, **266**, 118630.
4. J. Feng, H. Gao, L. Zheng, Z. Chen, S. Zeng, C. Jiang, H. Dong, L. Liu, S. Zhang and X. Zhang, *Nat. Commun.*, 2020, **11**, 4341.
5. B. Zhang, J. Zhang, J. Shi, D. Tan, L. Liu, F. Zhang, C. Lu, Z. Su, X. Tan, X. Cheng, B. Han, L. Zheng and J. Zhang, *Nat. Commun.*, 2019, **10**, 2980.
6. Y. Pan, R. Lin, Y. Chen, S. Liu, W. Zhu, X. Cao, W. Chen, K. Wu, W.-C. Cheong and Y. Wang, *J. Am. Chem. Soc.*, 2018, **140**, 4218-4221.
7. E. Zhang, T. Wang, K. Yu, J. Liu, W. Chen, A. Li, H. Rong, R. Lin, S. Ji and X. Zheng, *J. Am. Chem. Soc.*, 2019, **141**, 16569-16573.
8. F.Q. Yang, X.Y. Mao, M.F. Ma, C. Jiang, P.X. Zhang, J. Wang, Q. Deng, Z.L. Zeng and S.G. Deng, *Carbon*, 2020, **168**, 528-535.
9. Y. Zhang, L. Jiao, W. Yang, C. Xie and H.L. Jiang, *Angew. Chem., Int. Ed.*, 2021, **60**, 7607-7611.
10. S. Li, M. Ceccato, X. Lu, S. Frank, N. Lock, A. Roldan, X.-M. Hu, T. Skrydstrup and K. Daasbjerg, *J. Mater. Chem. A*, 2021, **9**, 1583-1592.
11. C. Zhao, X. Dai, T. Yao, W. Chen, X. Wang, J. Wang, J. Yang, S. Wei, Y. Wu and Y. Li, *J. Am. Chem. Soc.*, 2017, **139**, 8078-8081.
12. H. Zhong, F. Meng, Q. Zhang, K. Liu and X. Zhang, *Nano Research*, 2019, **12**, 2318-2323.

13. Z. Geng, Y. Cao, W. Chen, X. Kong, Y. Liu, T. Yao and Y. Lin, *Appl*. *Catal*., *B*, 2019, **240**, 234-240.
14. L. Jiao, W. Yang, G. Wan, R. Zhang, X. Zheng, H. Zhou, S. H. Yu and H. L. Jiang, *Angew*. *Chem*., *Int*. *Ed.*, 2020, **59**, 20589-20595.